**Grant Agreement No**.: 604656

**Project acronym**: NanoSim

**Project title**: A Multiscale Simulation-Based Design Platform for Cost-Effective $CO_2$ Capture Processes using Nano-Structured Materials (NanoSim)

**Funding scheme**: Collaborative Project

**Thematic Priority**: NMP

**THEME:** [NMP.2013.1.4-1] Development of an integrated multi-scale modelling environment for nanomaterials and systems by design

**Starting date of project**: 1st of January, 2014

**Duration**: 48 months

| WP N° | Del. N° | Title | Contributors | Version | Lead beneficiary | Nature | Dissemin. level | Delivery date from Annex I | Actual delivery date dd/mm/yyyy |
|---|---|---|---|---|---|---|---|---|---|
| 6 | D6.2 | Complete library of state of the art closure laws implemented into the code | Thomas Gurker<br>Joana Francisco Morgado | | 8 | D | PU | 24 | 25-01-2016 |

# 1 Description

The generic formulation of *Phenom* allows the simulation of fluidized bed reactors under the three regimes of fluidization which are more commonly used in industry (bubbling, turbulent and fast fluidization). Each of these regimes has its particular characteristic solid concentration profile (Figure 1).

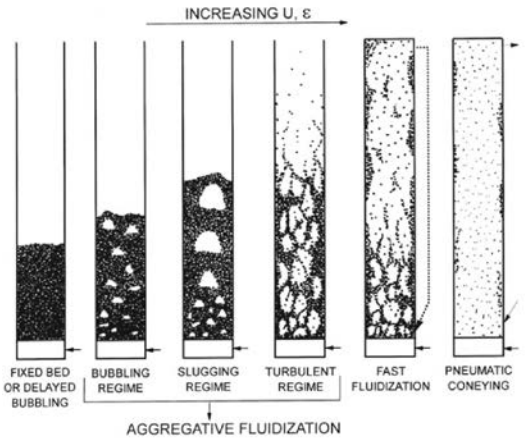


**Figure 1 – Gas-solid flow regime, Reference:** [1]

These profiles define the hydrodynamic of the reactor which in phenomenological models as *Phenom* are accomplished through closure laws from empirical and semi-empirical nature. The deliverable D6.2 consists of the implementation of a complete library of the state of the art closures into the code for the three fluidization regimes. This closures will be used to estimate the model parameters such as: the void fractions, the holdup and local phase void fractions; bubble size along the axial direction; bubble rise velocity; mass and heat transfer coefficients and the dispersion coefficients used to describe the mixing phenomena inside the reactor unit.

In the following a summary of the state of art material relations used in fluidized bed reactors modelling.

# 2 Bubbling Fluidization

The bubbling regime is the most studied fluidization regime in literature and it is characterized by lower inlet gas velocities ranging between 0.1 and 2 m $s^{-1}$[1]. These units operate above the called minimum fluidization velocity when large instabilities occur in the gas and solids flow with intense mixing between these two phases and presence of channeling of the gas (with low content of solids) through the bed (the so called bubbles).

The minimum fluidization velocity which determines the minimum conditions for fluidization is usually defined by (Grace 1982) a modification of (Wen and Yu 1966) through the following equation [2], [3]:

$$Re_{p,mf} = \sqrt{C_1^2 + C_2 Ar} + C_1 \quad (1)$$

The constants in Equation 1 take the following values: C1 = 27.2 and C2 = 0.0408 as proposed by (Grace 1982).

The understanding of the bubbling behavior is very important for determining the reactor efficiency. However, it is quite challenging since bubbles are subject to breakage and coalescence, phenomena that depend not only on the fluid velocity but also on the different types, sizes and distribution of solids in the rector. Many researchers have been working on finding expressions that can be used to estimate this complex behavior and in the current formulation of *Phenom* the library of closures for bubbling fluidization regime includes material relations for the following variables (Table 1).

**Table 1 – Variables defined though material relations under bubbling regime**

| Variable | Description | Units | Section |
|---|---|---|---|
| $d_b$ | Bubble size | [m] | 2.1 |
| $\varepsilon_{bubb}$ | Bed voidage under bubbling regime | [-] | 2.3 |
| $\varepsilon_{L_{bubb}}$ | Bed voidage in L-phase under bubbling regime | [-] | 2.4 |
| $K_{LH_{bubb}}$ | Mass transfer coefficient | [$s^{-1}$] | 2.5 |
| $\psi_{L_{bubb}}$ | Volume fraction of L-phase under bubbling regime | [-] | 2.6 |
| $D_{L_{bubb}}$ | Gas dispersion coefficient for L-phase | [$m^2\ s^{-1}$] | 2.7 |
| $D_{H_{bubb}}$ | Gas dispersion coefficient for H-phase | [$m^2\ s^{-1}$] | 2.7 |
| $\lambda_{bubb}$ | Thermal conductivity under bubbling fluidization | [$W\ m^{-1}\ K^{-1}$] | 2.8 |
| $u_{L_{bubb}}, U_b$ | Intrinsic gas velocity in L-phase under bubbling fluidization using the bubble rise velocity | [$m\ s^{-1}$] | 2.2 |

A description of the relations used to define the variables identified in Table 1 is given in the next sections.

## 2.1 Bubble size

The bubble size is one of the most important parameters in bubbling fluidized bed reactors since many other key parameters such as the bubble rise velocity, bubble fraction (L-phase fraction), interface transfer coefficient are dependent on it [4].

Several correlations have been developed to estimate the bubble size based on empirical data. Yasui and Johanson (1958) ([5], [6]) were among the first studying the bubble properties and deriving relations describing its growth. Later Darton (1977) developed a correlation which became very popular based on the bubbles coalescence and its trend to rise in preferred paths [7]. However, since breakage is not considering, this correlation has to be applied carefully (*e.g.* for Geldart A particles where large bubbles are only observed occasionally due to bubble splitting [8]). Reference [6] is a good review of the developed correlations for bubble size. In this study the evaluation of the different correlations is divided into different categories based on the Geldart classification of particles (Geldart A, B and D), superficial gas velocity (low and high velocity) and the distributor design (porous or perforated distributor) and the correlation results are compared against

experimental data. The most appropriate correlations under the different categories are presented in Table 2. Note that in terms of generality or wider range of application, the correlation of Mori and Wen is commonly suggested for a first rough estimation because it relates the bubble size with the bed diameter.

Table 2 - The best correlations for bubble size according to the study performed in [6]

| Category | Author(s) | Correlation | | Limitations |
|---|---|---|---|---|
| **Geldart A** | Cai et al. (1994) | $d_b = 0.138h^{0.8}(U_0 - U_{mf})^{0.42} exp\left(-2.5 \times 10^{-5}(U_0 - U_{mf})^2 - 10^{-3}(U_0 - U_{mf})\right)$ | (2) | Particle type: Different<br>$d_p$ (μm): 66-700<br>$\rho_p$ (g/cm$^3$): 0.85-3.186<br>$U_0$-$U_{mf}$ (cm/s): 0-0.6<br>$d_t$ (cm): 30x1; 30x20; 17x12; 13-38<br>Distributor: Porous and Perforated<br>Measuring type: Different |
| **Geldart B** | Choi et al. (1988) | $(U_0 - U_{mf})(d_b - d_0) + 0.474g^{0.5}(d_b^{1.5} - d_0^{1.5}) = 1.132(U_0 - U_{mf})h$ | (3) | Particle type: coal<br>$d_p$ (μm): 340-620<br>$\rho_p$ (g/cm$^3$): 2.3<br>$U_0$-$U_{mf}$ (cm/s): 4.7-17.1<br>$d_t$ (cm): 30x30<br>Distributor: Perforated<br>Measuring type: Electro-resistivity probe |
| | Mori and Wen (1975) | $\frac{d_{bm} - d_b}{d_{bm} - d_0} = \exp(-0.3h/d_t) d_{bm} = 1.87d_0$ | (4) | Particle type: Different<br>$d_p$ (μm): 60-450<br>$U_0$-$U_{mf}$ (cm/s):0-48<br>$d_t$ (cm):30-130<br>Distributor: Porous and Perforated<br>Measuring type: Different |
| **Geldart D** | Cai et al. (1994) | $d_b = 0.138h^{0.8}(U_0 - U_{mf})^{0.42} exp\left(-2.5 \times 10^{-5}(U_0 - U_{mf})^2 - 10^{-3}(U_0 - U_{mf})\right)$ | (2) | Particle type: Different<br>$d_p$ (μm): 66-700<br>$\rho_p$ (g/cm$^3$): 0.85-3.186<br>$U_0$-$U_{mf}$ (cm/s): 0-0.6<br>$d_t$ (cm): 30x1; 30x20; 17x12; 13-38<br>Distributor: Porous and Perforated<br>Measuring type: Different |
| **Low velocity** | Agarwal (1985, 1987) | $a = \frac{3.51(h + h_0)^{0.4}}{(d_t^{0.5} - d_0^{0.5})}$ | (5) | Particle type: Glass<br>$d_p$ (μm): 268<br>$U_0$-$U_{mf}$ (cm/s): 4.1-9.6 |

| | | | |
|---|---|---|---|
| | | For $a \leq 3$<br>$$d_b = d_0 + \frac{k_3}{11.13m} h^s d_0^{0.5} + \left(\frac{k_3}{22.26}\right)^2 \frac{h^{2s}}{m(m-1)}$$<br>$$k_3 = 82; m = 10;\ s = 0.4$$<br>For $a > 3$<br>$$d_b = \left[ d_0^{0.5} + 0.37(h+h_0)^{0.4} - 0.036(h+h_0)^{0.4} \left( \frac{1.17(h+h_0)^{0.4}}{d_t^{0.5} - d_0^{0.5}} - 1 \right) \right]^2$$ | $d_t$ (cm): 30x20<br>Distributor: Porous<br>Measuring type: X-ray photography |
| **High velocity** | Darton et al. (1977) | $$d_b = 0.54 g^{-0.2} (U_0 - U_{mf})^{0.4} (h + 4A_0^{0.5})^{0.8}$$ (6) | Particle type: different<br>$d_p$ (μm): 60-323<br>$\rho_p$ (g/cm$^3$): 0.6-2.65<br>$U_0$-$U_{mf}$ (cm/s): 0.5-20<br>$d_t$ (cm): 30x30; 30x20; 100, 61x61<br>Distributor: Porous<br>Measuring type: Capacitance probe, X-ray photography |
| **Perforated distributor** | Cai et al. (1994) | $$d_b = 0.138 h^{0.8} (U_0 - U_{mf})^{0.42} exp\left(-2.5 \times 10^{-5} (U_0 - U_{mf})^2 - 10^{-3}(U_0 - U_{mf})\right)$$ (2) | Particle type: Different<br>$d_p$ (μm): 66-700<br>$\rho_p$ (g/cm$^3$): 0.85-3.186<br>$U_0$-$U_{mf}$ (cm/s): 0-0.6<br>$d_t$ (cm): 30x1; 30x20; 17x12; 13-38<br>Distributor: Porous and Perforated<br>Measuring type: Different |
| **Porous distributor** | Choi et al. (1988) | $$(U_0 - U_{mf})(d_b - d_0) + 0.474 g^{0.5} (d_b^{1.5} - d_0^{1.5}) = 1.132 (U_0 - U_{mf}) h$$ (3) | Particle type: coal<br>$d_p$ (μm): 340-620<br>$\rho_p$ (g/cm$^3$): 2.3<br>$U_0$-$U_{mf}$ (cm/s): 4.7-17.1<br>$d_t$ (cm): 30x30<br>Distributor: Perforated<br>Measuring type: Electro-resistivity probe |

| | | | |
|---|---|---|---|
| | Mori and Wen (1975) | $\frac{d_{bm}-d_b}{d_{bm}-d_0}=\exp(-0.3h/d_t)d_{bm}=1.87d_0$ (4) | Particle type: Different<br>$d_p$ (µm): 60-450<br>$U_0$-$U_{mf}$ (cm/s):0-48<br>$d_t$ (cm):30-130<br>Distributor: Porous and Perforated<br>Measuring type: Different |

Other correlations commonly referred in literature are represented in Table 3.

**Table 3 – Bubble size correlations in bubbling fluidized beds** [4], [6]

| Author(s) | Correlation | Observations |
|---|---|---|
| Kato and Wen (1969) | $d_b=1.4\rho_p d_p\left(\frac{U}{U_{mf}}\right)h+d_0$ (7) | Particle type: Silica gel<br>$d_p$ (µm): 194<br>$\rho_p$ (g/cm$^3$): 1.4<br>$d_t$ (cm): 8.4<br>Distributor: Porous<br>Measuring type: Hot wire anemometer |
| Chiba et al. (1973) | $d_b=d_0\left(\frac{(2^{7/6}-1)(h-d_0)}{d_0}+1\right)^{2/7}$<br>$d_0=\left(6G/\pi k_b g^{1/2}\right)^{2/5}$ (8) | Particle type: Silica gel<br>$d_p$ (µm): 67-443<br>$d_t$(cm): 10,20<br>$k_b$ depends on the bed material and ranges between: 0.60-0.95 [4] |
| Rowe (1976) | $d_b=\frac{0.54\left(U-U_{mf}\right)^{1/2}(h+h_0)^{3/4}}{g^{1/4}}$ (9) | Particle type: Different<br>$d_p$ (µm): 135<br>$\rho_p$ (g/cm$^3$): 0.6<br>$U_0$-$U_{mf}$ (cm/s): 0.3-5.6<br>$d_t$ (cm): 30x1; 30x30<br>Distributor: Porous<br>Measuring type: X-ray photography |
| Darton et al. (1978) | $d_b=0.54g^{-0.2}\left(U-U_{mf}\right)^{0.4}\left(h+4\sqrt{A_0}\right)^{0.8}$ (10) | Particle type: Different<br>$d_p$ (µm): 60-323<br>$\rho_p$ (g/cm$^3$): 0.6-2.65<br>$U_0$-$U_{mf}$ (cm/s): 0.5-20<br>$d_t$ (cm): 30x1; 30x30, 30x20, 100, 61x61<br>Distributor: Porous |

| | | |
|---|---|---|
| | | Measuring type: X-ray photography, Capacitance probe |

Some correlations in Table 2 and Table 3 require the estimation an initial bubble size at the surface of the distributor, $d_0$. Some of the correlations developed for this purpose using different types of distributors are presented below.

**Table 4 - Bubble size at the bottom of the reactor (above the distributor)** [4]

| Author(s) | Correlation | Observations |
|---|---|---|
| Davidson and Harrison (1963) | $d_0 = 1.295G^{0.4}/g^{0.2}$ (11) | G: Volumetric flow rate of gas per orifice [4] |
| Kato and Wen (1969) | $d_0 = 1.295\left(\frac{U-U_{mf}}{N}\right)^{0.4}/g^{0.2}$ (12) | Correlation developed for perforated plates.<br>N: Number of orifices per unit area |
| Geldart (1972) | $d_0 = 1.43\left(\frac{U-U_{mf}}{N}\right)^{0.4}/g^{0.2}$ (13) | Correlation developed for perforated plate but for porous plates we can use N = 0.1 hole/cm$^2$ of bed cross section [6] |
| Chiba et al. (1972) | $d_0 = 1.259\left(\frac{G}{k_b}\right)^{0.4}/g^{0.2}$ (14) | $k_b$ depends on the bed material and ranges between: 0.60-0.95 |
| Miwa et al. (1972) | Perforated plate: $d_0 = 0.347\left(\frac{U-U_{mf}}{N}\right)^{0.4}$ (15)<br>Porous plate: $d_0 = 0.00376\left(U-U_{mf}\right)^2$ | |
| Fryer and Potter (1976) | $d_0 = 1.08\left(U-U_{mf}\right)^{0.33}$ (16) | |
| Darton et al. (1977) | $d_0 = 1.63\left(\left(U-U_{mf}\right)A_0/g^{1/2}\right)^{2/5}$ (17) | $A_0$: the area of plate per hole<br>For porous plate $A_0$=0.56 cm$^2$ |

The maximum bubble diameter it is still not resolved, however a good rough estimation of this parameter $d_{bm}$ can be made using the following equation[4].

$$d_{bm} = 2U_t^2/g$$

## 2.2 Bubble rise velocity

The study performed in [6] also evaluates correlations developed for the bubble rise velocity. Based on the squared differences (to be minimized) the correlation of Werther represents the best overall coverage for different particles. It is important to refer that the bubble rise velocity is highly dependent on the type of the particles therefore different expressions are commonly used for the different Geldart particles type instead of a single generic correlation. The correlations that show better results according to [6] are given in Table 3. The most popular correlation in literature is the simple closure developed by Davidson and Harrison.

Table 5 - The best correlations for bubble rise velocity according to the study performed in [6]

| Category | Author(s) | Correlation | Limitations |
|---|---|---|---|
| Generic | Werther (1978) | $U_b = \psi\sqrt{g d_b}$<br>Geldart A (FCC):<br>$\psi = \begin{cases} 1 & d_t \le 10 \\ 0.396 {d_t}^{0.4} & 10 < d_t < 100 \\ 2.5 & d_t \ge 100 \end{cases}$ (18)<br>Geldart B (sand):<br>$\psi = \begin{cases} 0.64 & d_t \le 10 \\ 0.254 {d_t}^{0.4} & 10 < d_t < 100 \\ 1.6 & d_t \ge 100 \end{cases}$ | Particle type: FCC, sand<br>$d_p$ (μm): 60, 130<br>$\rho_p$ (g/cm$^3$): 1200,2640<br>$U_0$-$U_{mf}$ (cm/s): 4-29<br>$d_t$ (cm): 45, 100<br>Distributor: Porous<br>Measuring type: Capacitance probe |
| Generic | Davidson and Harrison (1972) | $U_b = U_{br} + (U_0 - U_{mf})$ (19) | |
| **Geldart A** | Hilligardt and Werther (1986) | $U_b = \psi(U_0 - U_{mf}) + \vartheta U_{br}$<br>Geldart A:<br>$\psi = 0.8$<br>$\vartheta = 0.7 {d_t}^{1/3}$<br>Geldart B: (20)<br>$\psi = \begin{cases} 0.67 & z/d_t < 1.7 \\ 0.51(z/d_t)^{1/2} & 1.7 \le z/d_t \le 4 \\ 1 & z/d_t > 4 \end{cases}$<br>$\vartheta = 0.2 {d_t}^{1/2}$<br>Geldart D: | Particle type: FCC, sands, quatz<br>$d_p$ (μm): 60-1300<br>$\rho_p$ (g/cm$^3$): 1200-2640<br>$U_0$-$U_{mf}$ (cm/s): 5-30<br>$d_t$ (cm): 30x200; 50x50; 100x100<br>Distributor: Porous<br>Measuring type: Capacitance probe |

| | | | |
|---|---|---|---|
| | | $\psi = \begin{cases} 0.26 & z/d_t < 0.55 \\ 0.35(z/d_t)^{1/2} & 0.55 \le z/d_t \le 8 \\ 1 & z/d_t > 8 \end{cases}$ <br> $\vartheta = 0.87$ | |
| **Geldart B** | Davidson and Harrison (1972) | $U_b = U_{br} + (U_0 - U_{mf})$ (19) | |
| **Geldart D** | Werther (1978) | $U_b = \psi\sqrt{g d_b}$ <br> Geldart A (FCC): <br> $\psi = \begin{cases} 1 & d_t \le 10 \\ 0.396 {d_t}^{0.4} & 10 < d_t < 100 \\ 2.5 & d_t \ge 100 \end{cases}$ (18) <br> Geldart B (sand): <br> $\psi = \begin{cases} 0.64 & d_t \le 10 \\ 0.254 {d_t}^{0.4} & 10 < d_t < 100 \\ 1.6 & d_t \ge 100 \end{cases}$ | Particle type: FCC, sand<br>$d_p$ (µm): 60, 130<br>$\rho_p$ (g/cm$^3$): 1200,2640<br>$U_0$-$U_{mf}$ (cm/s): 4-29<br>$d_t$ (cm): 45, 100<br>Distributor: Porous<br>Measuring type: Capacitance probe |

The parameter $U_{br}$ corresponds to the bubble rise velocity for single bubbles. Several correlations have been proposed to define this parameter but the simple Davidson and Harrison (1963) is still the most popular in literature. Table 4 represents some of the other correlations. According to the study conducted in reference [6] the more appropriate and generic correlations are the correlations of Allahwala and Potter and Wallis since they take into account the effect of the bed diameter on the bubble rise velocity.

**Table 6 – Correlations of single bubble rise velocity** [6], [8]

| Author(s) | Correlation | | Remarks |
|---|---|---|---|
| Davidson and Harrison (1963) | $U_{br} = 0.71\sqrt{gd_b}$ | (21) | |
| Rowe and Partridge | $U_{br} = k\sqrt{gd_b}$<br>$k = 0.926$ for Geldart A<br>$k = 1.02$ for Geldart B | (22) | $d_p$ (μm): 52-550<br>$\rho_p$ (g/cm$^3$): 1120-2930<br>$U_{mf}$(cm/s): 0.32-25.9<br>$d_t$ (cm): 14<br>Measuring type: X-ray photography |
| Wallis | $U_{br} = \left(0.711\sqrt{gd_b}\right)1.2exp\left(-1.49\frac{d_b}{d_t}\right)$ | (23) | |
| Allahwala and Potter | $U_{br} = 0.35\sqrt{gd_t}tan^{0.555}\left(3.6\left(\frac{d_b}{d_t}\right)^{0.9}\right)$ | (24) | $d_p$ (μm): 59, 68, 198<br>$U_{mf}$(cm/s): 0.89-3.74<br>$d_t$ (cm): 24, 4, 61<br>Measuring type: X-ray photography |

## 2.3 Bed voidage (hold-up)

The voidage or total voidage along the height of the reactor is commonly described by the correlation defined by Clift and Grace (1985) given below [9], [10].

$$\varepsilon = \frac{1-(1-\varepsilon_{mf})}{\left(1+\frac{U-U_{mf}}{0.711\sqrt{gd_b}}\right)} \tag{25}$$

The void at minimum fluidization conditions, $\varepsilon_{mf}$, is determined using the expression proposed by Grace (1986) [2].

$$\varepsilon_{mf} = 0.586Ar^{-0.029}\left(\frac{\rho_g}{\rho_s}\right)^{0.021} \tag{26}$$

## 2.4 Bed voidage in L-phase

The void fraction of the bubbles or low density phase has still not been resolved [10]. Many models in literature assume this parameter to be equal to 1 because the amount of solids inside these pockets of gas is much lower compared to the amount of solids present in the high density phase. However, this assumption is poor and can have some impact on the reactor performance since reaction also occurs on the low density phase and can be significant when fast reactions are taking place. Therefore a value of 0.97 is used in Phenom as other authors have done [10], [11].

## 2.5 Mass transfer coefficient

Several correlations have been proposed in literature for defining the mass transfer coefficient (or gas interchange coefficient) between the L- and H- phases in bubbling beds, $K_{LH_{bubb}}$. The interchange coefficient can be defined as the flow of gas from bubble to emulsion with an equal flow in the opposite direction as represented below [8] and in Figure 2.

$$K_{LH_{bubb}} = \frac{\text{volume of gas bubble} \rightarrow \text{emulsion or emulsion} \rightarrow \text{bubble}}{(\text{volume of bubbles in the bed})(\text{time})}$$

This parameter is very important for determining the reactor performance since it may limit the conversion in some reactors. It gives the rate through which the reactants are transferred from/to the L-phase poor in solids to/from the H-phase where the solid-gas contact is excellent.

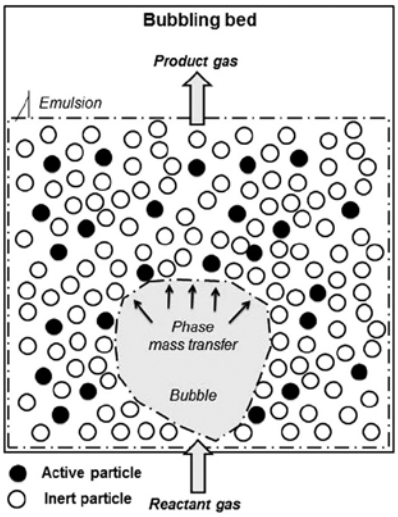


**Figure 2 - Scheme of the Interphase mass transfer in bubbling fluidized bed Source:** [13]

A very popular correlation is the one proposed by Sit and Grace (1985) (Equation 27) for spherical, three-dimensional bubbles which considers interaction (coalescence) between the bubbles [9], [10], [12].

$$K_{LH_{bubb}} = \left(\frac{U_{mf}}{3} + 2\left(\frac{D_i \varepsilon_{mf} U_H}{\pi d_b}\right)^{1/2}\right)\frac{6}{d_b} \quad (27)$$

The Equation 27 considers two mechanisms for the interphase mass transfer, throughflow (or convection) and diffusion mechanisms which are represented in the two terms of the expression, respectively [12], [13]. Therefore, the first term proportional to the minimum fluidization velocity, $U_{mf}$, corresponds to the convective term and results from Murray's hydrodynamic analysis of bubbles in fluidizes beds [12], [14] and the second term to the diffusion mechanism and is derived from the penetration theory ($K_{LH_{bubb}} \propto D^{1/2}$)[1], [12]. Some other mass transfer coefficient correlations are presented in Table 4.

**Table 7 – Correlations for the mass transfer coefficient under bubbling regime often referred in literature**[8], [12], [13]

| Author(s) | Correlation | Observations |
|---|---|---|
| Davidson and Harrison (1963) | $K_{LH_{bubb}} = 0.75U_{mf} + 0.975\left(\frac{D^{1/2}g}{d_b^{1/4}}\right)^{1/4}$ (28) | |
| Chiba and Kobayashi (1970) | $K_{LH_{bubb}} = 1.128\left(\frac{\varepsilon_{mf}^2 D U_b}{d_b}\right)^{1/2}\left(\frac{\alpha-1}{\alpha}\right)^{2/3}$ (29) | $d_t$ (cm): 10<br>$d_p$ (μm): 140-210<br>U(cm/s): ~ $U_{mf}$<br>$U_{mf}$ (cm/s): 3.1-5 |
| Davidson et al. (1977) | $K_{LH_{bubb}} = 1.19U_{mf} + 0.91\left(\frac{D^{1/2}g^{1/4}}{d_b^{1/4}}\right)\frac{\varepsilon_{mf}}{1+\varepsilon_{mf}}$ (30) | |
| Sit and Grace (1985) | $K_{LH_{bubb}} = \left(\frac{U_{mf}}{3} + 2\left(\frac{D\varepsilon_{mf}U_b}{\pi d_b}\right)^{1/2}\right)\frac{6}{d_b}$ (27) | Equation for spherical three-dimensional bubbles in freely bubbling beds.<br>Particle type: glass beads<br>Tracer: Ozone<br>$d_p$ (μm): 390 |
| Sit and Grace (1985) | $K_{LH_{bubb}} = \left(0.4U_{mf} + \left(\frac{4D\varepsilon_{mf}U_b}{\pi d_b}\right)^{1/2}\right)\frac{6}{d_b}$ (31) | Equation for circular two-dimensional bubbles in freely bubbling beds.<br>Particle type: glass beads<br>Tracer: Ozone<br>$d_p$ (μm): 390 |
| Kunii and Levenspiel (1991) | $\frac{1}{K_{LH_{bubb}}} = \frac{1}{K_{bc}} + \frac{1}{K_{ce}}$ (32)<br>$K_{bc} = 4.5\left(\frac{U_{mf}}{d_b}\right) + 5.85\left(\frac{D^{1/2}g^{1/4}}{d_b^{5/4}}\right)$ (33)<br>$K_{ce} = 6.77\left(\frac{D\varepsilon_{mf}U_b}{d_b^3}\right)^{1/2}$ (34) | Particle type: particles of type Geldart A |

## 2.6 Volume fraction of L-phase

The volume fraction in the low density phase is determined by a simple mass balance given as follows (Equation 37).

$$U_0 = \varphi_L \varepsilon_L u_L + \varphi_H \varepsilon_H u_H \quad (35)$$

$$U_0 = \varphi_L (\varepsilon_L u_L - \varepsilon_H u_H) + \varepsilon_H u_H \quad (36)$$

$$\varphi_L = \frac{U - \varepsilon_H u_H}{\varepsilon_L u_L - \varepsilon_H u_H} \quad (37)$$

## 2.7 Axial gas dispersion coefficient

The study of the gas mixing in bubbling fluidized beds dates from 1945 with Gilliland and Mason. The understanding of the gas dispersion phenomena inside the bed is very important for describing the flow pattern but also for determining the reactor performance.

Abba (2001) conducted steady and unsteady state tracer measurements using helium for determining the dispersion coefficient under bubbling and turbulent fluidization regimes. It was verified that the dispersion in the L-phase is considered negligible compared with the H-phase so he suggested it can be approximated by the molecular diffusivity of the gas (at lower velocities) by Equation 38. As the superficial gas velocity increases this difference between the dispersion coefficients is tightened [11].

The dispersion coefficient for L-phase under bubbling regime is then estimated by the averaged molecular diffusivity of the gas mixture (Equation 38).

$$D_{L_{bubb}} = D_{mix} = \sum_{i=1}^{N_{comp}} w_{i,L} \, D_{i_{L_{bubb}}} \quad (38)$$

Where $D_{i_{L_{bubb}}}$ corresponds to the diffusivity of component *i* in the gas mixture is determined by the Wilke model (mass basis) which was also applied in the *Generic Fluidized Bed Reactor model* [9], [10].

$$D_{i_{L_{bubb}}} = \frac{1 - w_{i,L}}{\bar{M} \sum_{\substack{i=1 \\ j \neq i}}^{N_{comp}} \frac{w_{j,L}}{M_j D_{ij}}} \quad (39)$$

The binary diffusivity, $D_{ij}$, is determined by the semiempirical method of Fuller *et al.* (1966)[15] using atomic diffusion volumes for each gas molecule (Equation 40).

$$D_{ij} = \frac{1.00 \times 10^{-1} T^{1.75} \left(1/M_i + 1/M_j\right)^{1/2}}{P \left[\left(\sum v_i\right)^{1/3} + \left(\sum v_j\right)^{1/3}\right]^2} \quad (40)$$

The dispersion coefficient for H-phase is defined using the correlation proposed by Bi et al. (2000) [16] obtained from a large pool of literature data for axial gas dispersion coefficients (Cankurt and Yerushalmi (1978), Li and Wu (1991), Foka *et. al* (1996), among others)[16].

$$D_{H_{bubb}} = \frac{U_H H}{Pe_{bubb}} \tag{41}$$

$$Pe_{bubb} = 3.472 Ar^{0.149} Re^{0.0234} Sc^{-0.231} \left(\frac{H}{d_t}\right) \tag{42}$$

## 2.8 Thermal conductivity

Matsen (1985) [17] proposed the thermal conductivity of the fluidized bed to be estimated as follows.

$$\lambda_{bubb} = (1-\varepsilon)\rho_s C_{p,s} D_{s_{bubb}} \tag{43}$$

The axial dispersion coefficient for solids to be used in the previous equation is defined by the correlation proposed by Lee and Kim (1990) in terms of Peclet and Archimedes number as follows [18].

$$D_{s_{bubb}} = 1.058(U_0 - U_{mf}) d_t \left(\frac{g d_t}{U_0 - U_{mf}}\right)^{0.653} Ar^{-0.368} \tag{44}$$

Equation 43 covers Froude numbers, $Fr_t$, and Archimedes numbers, Ar, in the ranges $8.0\text{x}10^{-4}$- 0.91 and 6.9 – 72.4, respectively.

# 3 Turbulent fluidization

In turbulent and fast fluidization regimes the formation of bubbles is mainly inexistent (a disappearance of large voids/bubbles is verified) therefore neither the bubble size nor bubble rise velocity are defined for these regimes [1], [8], [16]. The model parameters described in Table 8 are described through material relations.

Table 8 – Variables defined though material relations under turbulent regime

| Variable | Description | Units | Section |
|---|---|---|---|
| $\varepsilon_{turb}$ | Bed voidage under turbulent regime | [-] | 3.1 |
| $\varepsilon_{L_{turb}}$ | Bed voidage in L-phase under turbulent regime | [-] | 3.3 |
| $K_{LH_{turb}}$ | Mass transfer coefficient | [ $s^{-1}$] | 3.4 |
| $\psi_{L_{turb}}$ | Volume fraction of L-phase under turbulent regime | [-] | 3.5 |
| $D_{L_{turb}}$ | Gas dispersion coefficient for L-phase | [$m^2$ $s^{-1}$] | 3.6 |
| $D_{H_{turb}}$ | Gas dispersion coefficient for H-phase | [$m^2$ $s^{-1}$] | 3.6 |
| $\lambda_{turb}$ | Thermal conductivity under turbulent fluidization | [W $m^{-1}$ $K^{-1}$] | 3.7 |
| $u_{L_{turb}}, U_b$ | Intrinsic gas velocity in L-phase under turbulent fluidization | [m $s^{-1}$] | 3.2 |

## 3.1 Bed voidage

Several researchers have investigated the bed density behavior under turbulent regime. Some authors considered distinct phases as in the bubbling regime and others used only a single phase since the bubbles vanish rapidly (bubbles are present only at low velocities and are characterized by smaller sizes compared to bubbling regime). Considering the dense bed, as the velocity increases in the turbulent regime, the volume fraction of voids increases with size dependent on the mechanisms of coalescence and splitting [16]. Therefore, the suspension becomes more uniform at higher velocities. Due to high fluctuations in the velocity (inherent to the turbulent regime), empirical approaches play a very important role in describing the reactor hydrodynamics in turbulent regime. Equation 46 commonly used to characterize the reactor was derived by King (1989) by extensive experience in catalytic cracking process (FCC)[19], [20].

Table 9 – Void fraction in turbulent fluidized bed reactors

| Author(s) | Correlation | | Observations |
|---|---|---|---|
| Avidan (1980) | $\frac{U}{U_t^*} = \varepsilon^n$ | (45) | Improvement of Richadson-Zaki equation where $U_t^*$ corresponds to the effective terminal cluster velocity [16], [20]. |
| King (1989) | $\varepsilon = \frac{U+1}{U+2}$ | (46) | Based on extensive experience in FCC process. [20]. |

Some authors that consider the presence of bubbles have developed new correlations [16]. The main authors and studies conducted to determine this parameter are summarized in [16] in Table 7.

## 3.2 Gas velocity in L-phase

As mentioned earlier, under fast fluidization conditions the formation of bubbles can be neglected. Therefore, the gas velocity at the L-phase corresponds to the superficial velocity of the gas[9], [10].

$$u_{L_{turb}} = U_b = \frac{U_0}{\varepsilon} \tag{47}$$

## 3.3 Bed voidage in L-phase

$\varepsilon_{L_{turb}}$ can then be described by the total bed void fraction (Equation 46) [9], [10].

## 3.4 Mass transfer coefficient

One of the advantages of operating under fast fluidization regime relies on the enhancement of the interphase mass transfer that may dominant under bubbling regime. Some correlations have been reported in literature describing this parameter and the ones that are most often referred are summarized in Table 10.

Table 10 - Correlations for the mass transfer coefficient under turbulent regime[13], [16]

| Author(s) | Correlation | | Observations |
|---|---|---|---|
| Miyauchi et al. (1980) | $K_{LH_{turb}} = k_g a_I = 3.7 \frac{D_{turb}^{1/2} \psi_L}{d_b^{5/4}}$ | (48) | This expression considers the presence of bubbles.<br>$K_{LH_{turb}}$ ($s^{-1}$) : 0.8 – 1<br>$U_0$(m/s): 0.2-0.5<br>$d_p$ (µm): 53 |
| Foka et al. (1996) | $K_{LH_{turb}} = k_g a_I = 1.631 Sc^{0.37} U_0$ | (49) | A 2-phase model of van Deemter was used to determine the coefficient.<br>$K_{LH_{turb}}$ ($s^{-1}$) : 0.19-4.6<br>$U_0$(m/s): bubbling and turbulent regime up to 2.6 m/s<br>$d_p$ (µm): 53 |
| Zang and Quian (1997) | $k_g = 1.74 \times 10^{-4} Sc^{0.81} \frac{D_{turb}}{d_p}$ | (50) | 2-phase model with dispersion and steady-state point-source tracer injection technique was used to determine the coefficient.<br>$U_0$(m/s): 0.4-1<br>$d_t$(m): 0.2<br>H(m): 5<br>$d_p$ (µm): 77 (FCC particles) |

The correlation proposed by Foka et al. is the most generic since it is valid under a widest range of operating conditions (gas superficial velocities up to 2.6 m/s).

## 3.5 Volume fraction of L-phase

The volume fraction is determined the same way as in the bubbling regime (Equation 51)[9], [10].

$$\varphi_{L_{bubb}} = \varphi_{L_{turb}} = \frac{U - \varepsilon_H u_H}{\varepsilon_L u_L - \varepsilon_H u_H} \tag{51}$$

## 3.6 Axial gas dispersion coefficient

Some researchers have studied the axial gas dispersion using steady and unsteady tracer measurements using different tracers. A summary of the studies referred in literature can be found in reference [16]. Due to the limitations (or narrow range of application) of the correlations resulting from the studies published in literature, Bi et al. (2000) proposed a new correlation that comprises a wide collection of literature data (Equation 52)[16]. Equation 52 is used for defining the axial dispersion in *Phenom* under turbulent and bubbling regimes.

$$Pe_{turb} = Pe_{bubb} = 3.472 Ar^{0.149} Re^{0.0234} Sc^{-0.231} \left(\frac{H}{d_t}\right)$$
$$D_{L_{turb}} = \frac{U_0 H}{Pe_{turb}} \tag{52}$$

$$D_{H_{turb}} = \frac{U_H H}{Pe_{turb}}$$

## 3.7 Thermal conductivity

The thermal conductivity coefficient is defined the same way as in bubbling regime and the axial dispersion coefficient for solids required in Matsen's approach is also described by the same correlation (Equation 44) since it is valid for both regimes.

$$D_{s_{turb}} = D_{s_{bubb}} = 1.058(U_0 - U_{mf})d_t \left(\frac{g d_t}{U_0 - U_{mf}}\right)^{0.653} Ar^{-0.368} \quad (53)$$

# 4 Fast Fluidization

The fast fluidization regime is characterized by high velocities and a continuous decrease of solids content over the height of the reactor (the dense bed and freeboard are indistinguishable). Several models have been proposed for fast fluidization fluidized bed reactor. The two zone core-annulus model is the most realistic model because it considers a more dilute phase in the core and a denser phase in the annulus where the particles tend to accumulate and move downwards. The core-annulus model is used in *Phenom* under fast fluidization conditions therefore the correlations presented below are consistent with this formulation. The parameters described through these correlations are presented in Table 11.

Table 11 - Variables defined though material relations under fast fluidization regime

| Variable | Description | Units | Section |
|---|---|---|---|
| $\varepsilon_{fast}$ | Bed voidage under turbulent regime | [-] | 4.1 |
| $\varepsilon_{L_{fast}}$ | Bed voidage in L-phase under turbulent regime | [-] | 4.3 |
| $K_{LH_{fast}}$ | Mass transfer coefficient | [$s^{-1}$] | 4.4 |
| $\psi_{L_{fast}} = \psi_c$ | Volume fraction of core zone | [-] | 4.5 |
| $D_{L_{fast}}$ | Gas dispersion coefficient for L-phase | [$m^2 s^{-1}$] | 4.6 |
| $D_{H_{fast}}$ | Gas dispersion coefficient for H-phase | [$m^2 s^{-1}$] | 4.6 |
| $\lambda_{fast}$ | Thermal conductivity under turbulent fluidization | [$W m^{-1} K^{-1}$] | 4.7 |
| $u_{L_{fast}}, U_b$ | Intrinsic gas velocity in L-phase under turbulent fluidization | [$m s^{-1}$] | 4.2 |

## 4.1 Bed voidage

The solids flux and gas velocity are related by the following expression.

$$G_s = \rho_p(1-\varepsilon)\left(\frac{U_0}{\varepsilon} - U_{slip}\right) \quad (54)$$

Where the average particle velocity, $U_s$ is defined in terms of the slip velocity between the gas and solid, $U_{slip}$.

$$U_s = \frac{U_0}{\varepsilon} - U_{slip} \tag{55}$$

The slip velocity is usually considered to be equal to the terminal velocity of the particle. However, Patient et al. (1992) concluded that a more adequate relation is needed to better describe the relationship between the solids and the gas [21]. A called slip factor, φ, consisting ofthe ratio between the actual gas velocity and the particle velocity, was then introduced.

$$\varphi = \frac{U_0}{\varepsilon U_s} \tag{56}$$

Substituting Equation 55 in 54 and using the slip factor as defined by Equation 56 the following relationship is obtained for the void fraction along the bed of the reactor.

$$\varepsilon_{fast} = \varepsilon = \left[1 + \frac{G_s \varphi}{\rho_p U_0}\right]^{-1} \tag{57}$$

Matsen found that the slip factor approximately equals to 2 under fully developed flow regimes in risers (for gas velocities higher than 6 m/s)[21]. Based on this and by evaluating more literature data Patient et al. (1992) proposed a new correlation that relates better the gas and solids velocities[21].

$$\varphi = 1 + \frac{5.6}{Fr} + 0.47 Fr_t^{0.41} \tag{58}$$

## 4.2 Gas velocity in L-phase

The gas velocity in the L-phase is determined by the following expression which agrees with the core-annulus model.

$$u_{L_{turb}} = U_b = \frac{U_0}{\psi_c} \tag{59}$$

## 4.3 Bed voidage in L-phase

Since most of the gas flows through the core zone (L-phase), the voidage in this phase equals to the total bed void defined in section 4.1 by Equations 57 and 58.

## 4.4 Mass transfer coefficient

The interphase mass transfer coefficient between the two zones (core and annulus) has been studied by several researchers (Figure 3). Some of the proposed correlations are given in Table 12.

| Authors | $D$ m | $H$ m | $d_p$ μm | $\rho_p$ kg/m$^3$ | $U$ m/s | $G_s$ kg/m$^2$s | Tracer/ reactant | Method | $K_{ca}$ m/s | $2K_{ca}/R$ 1/s |
|---|---|---|---|---|---|---|---|---|---|---|
| Brereton et al. (1988) | 0.15 | 9.3 | 148 | 2650 | 7.1 | 0–65 | He | Pulse | 0.08–0.11 | 2.1–2.9 |
| Werther et al. (1992) | 0.14 | 8.5 | 130 | 2600 | 3 | 0–30 | $CO_2$ | Steady state | 0.02–0.1 | 0.8–4.0 |
| White et al. (1992) | 0.09 | 7.2 | 71 | 1375 | 2–8 | 0–280 | Ar | Pulse | 0.015–0.06 | 0.7–2.7 |
| Patience and Chaouki (1993) | 0.083 | 5 | 277 | 2630 | 4–8 | 20–140 | Ar | Pulse | 0.031–0.11 | 1.5–5.0 |
| Namkung and Kim (1998) | 0.10 | 5.3 | 65 | 1720 | 2.5–4.5 | 0–53 | He, $CO_2$ | Steady state | 0.1–0.3 | 4.0–12.0 |
| Kagawa et al. (1991) | 0.10 | N/A | 46 | 2300 | 3 | 0–80 | $O_3$ | Reaction | 0.002 | 0.08 |
| Bi et al. (1991) | 0.10 | 6.1 | 55 | 1500 | 1.5–2.5 | 0–25 | $O_3$ | Reaction | 0.001–0.003 | 0.04–0.12 |
| Ouyang et al. (1993) | 0.25 | 10 | 75 | 1700 | 2–8 | 0–400 | $O_3$ | Reaction | 0.001–0.002 | 0.04–0.12 |

Figure 3 – Important studies on the interphase gas coefficients between core and annulus phases. Source: [22]

Table 12 – Interphase mass transfer correlations between core and annulus

| Author(s) | Correlation | | Remarks |
|---|---|---|---|
| Pugsley et al. (1992) | $K_{LH_{fast}} = k_g a_I = \left[\frac{4D_{fast}\varepsilon_a U}{\pi H}\right]^{0.5} \times \frac{2}{r_c}$ | (60) | Uses the Higbie penetration theory and was validated by G. S. Patience by RTD measurements[23]. |
| Patience and Chaouki (1993) | $\frac{k_g d_t}{D_{fast}}\left(\frac{r_c}{R}\right) = 0.25 Sc^{0.5} Re^{0.75} \left[\frac{G_s}{\rho_s U_0}\right]^{0.25}$ | (61) | |

In the current formulation of *Phenom* Equation 60 is being used to describe the interphase mass transfer between the core and the annulus phases[9], [10].

## 4.5 Volume fraction of L-phase

According to the core-annulus model as represented in Figure 3 the L-phase corresponds to the core zone. Therefore the L-phase volume fraction is determined by the following expression.

$$\psi_{L_{fast}} = \psi_c = \frac{r_c^2}{R^2} \quad (60)$$

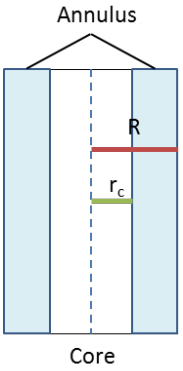


Figure 4 - Core-annulus model sketch

Where the core radius is given by a correlation developed by Bi et al. (1996) as a result of a least squares fitting of literature data [10], [22].

$$r_c = \frac{d_t}{2} - \frac{d_t}{2}\left(1 - \left(1.34 - 1.3\left(1 - \varepsilon_{fast}\right)^{0.2} + \left(1 - \varepsilon_{fast}\right)^{1.4}\right)\right)^{0.5} \quad (61)$$

## 4.6 Axial gas dispersion coefficient

Some studies have been conducted to determine the axial das dispersion coefficient under fast fluidization regime. Most of these studies are performed in circulating fluidized beds which commonly operate under this regime. Breault (2006) summarized some of these studies which are represented in Figure 5.

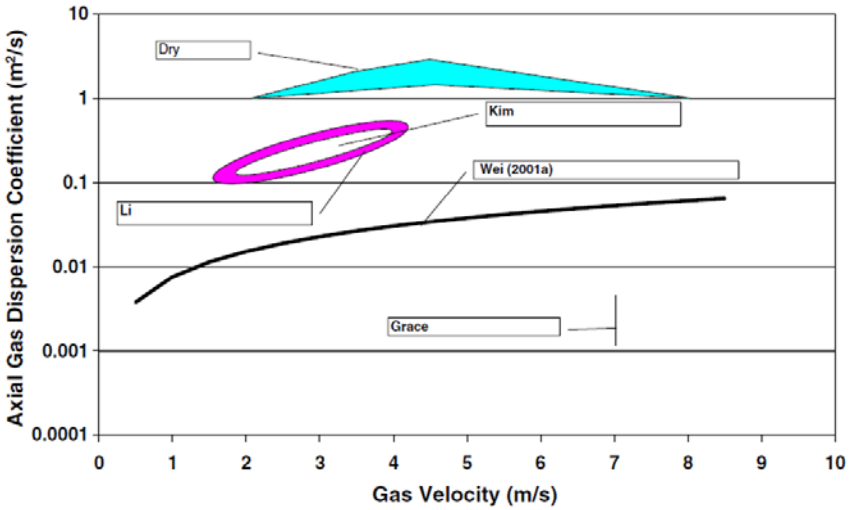


Figure 5 – Axial gas dispersion coefficients referred in literature. Source: [24]

Some of the developed correlations are presented in Table 13.

Table 13 – Axial gas dispersion coefficient correlations for fast fluidization regime

| Author(s) | Correlation | |
|---|---|---|
| Grace et al.(1988) | $D_{fast} = 7.1 \times 9.3 \times f(dP)$<br>$1 < D_{fast} < 11.8$<br>$Pe = f(dP)$ | (62) |
| Li and Wu (1991) | $D_{fast} = 0.184\varepsilon_{fast}^{-4.445}$ | (63) |

The correlation proposed by Li and Wu is used in Phenom as in [9], [10].

$$D_{L_{fast}} = D_{H_{fast}} = 0.184\varepsilon_{fast}^{-4.445} \quad (64)$$

## 4.7 Thermal conductivity

The thermal conductivity for fast fluidization is also defined by the Matsen's approach (see section 2.8) therefore correlations for the gas dispersion are required. Table 14 presents the correlations that are more commonly referred in literature also represented in Figure 6 .

Table 14 – Correlations for the axial dispersion coefficient for the solid particles[24]–[26]

| Author(s) | Correlation | | Remarks |
|---|---|---|---|
| Wei et al. (1998) | $D_{s_{fast}} = 0.0139 H U_0 (1-\varepsilon_{fast})^{-0.67} Re^{-0.23}$ | (65) | Particle type: fluorescing Particles (alumina particles with fine phosphor particles, less than 10 μm)<br>$d_p$ (μm): 54<br>$\rho_p$ (kg/m$^3$): 1710<br>$G_s$ (kg/m$^2$ s): 3-160<br>$U_0$ (m/s): 2.67-7.84<br>$d_t$ (cm): 12x120<br>Measuring type: |
| Chaouki et al. (1999) | $D_{s_{fast}} = 0.9$ | (66) | Particle type: Radioactive gold particles (tracer) with silica<br>$d_p$ (μm): 500<br>$G_s$ (kg/m$^2$ s): 23-75<br>$U_0$ (m/s) =4<br>$d_t$ (cm): 82x700<br>Measuring type: Radioactive Particle Tracking (RPT) |

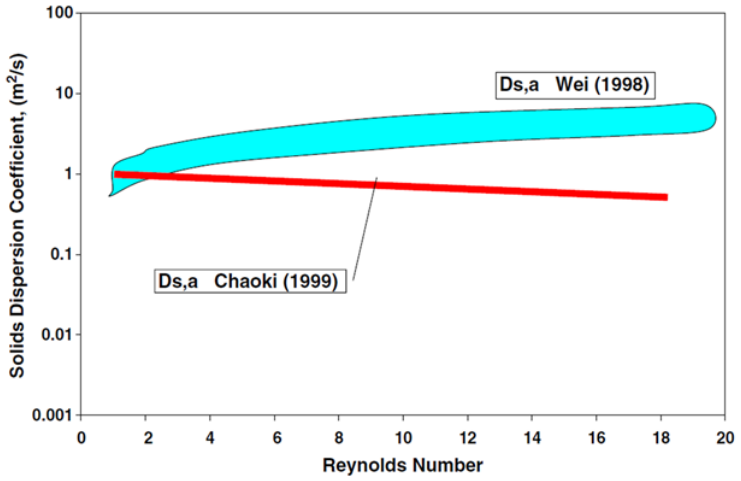


Figure 6 – Solid dispersion coefficient for fast fluidization regime. Source: [24]

In Phenom is used the correlation of Wei et al. (1998) which is also applied in [10].

## References

[1] H. A. Jakobsen, *Chemical Reactor Modeling Multiphase Reactive Flows*, Second. Springer, 2014.

[2] A. Abad, J. Adánez, F. García-Labiano, L. F. de Diego, and P. Gayán, "Modeling of the chemical-looping combustion of methane using a Cu-based oxygen-carrier," *Combust. Flame*, vol. 157, no. 3, pp. 602–615, Mar. 2010.

[3] C. Y. Wen and Y. H. Yu, "A generalized method for predicting the minimum fluidization velocity," *AIChE J.*, vol. 12, no. 3, pp. 610–612, 1966.

[4] C. Y. Wen, "Flow regimes and flow models for fluidized bed reactors. In L.K. Doraiswamy(Ed)," in *Recent advances in the engineering analysis of chemically reacting systems*, New Deli: Wiley Eastern, 1984, pp. 256–290.

[5] G. Yasui and L. N. Johanson, "Characteristics of Gas Pockets in Fluidized Beds," *AIChE J.*, vol. 4, no. 4, pp. 445–452, 1958.

[6] S. Karimipour and T. Pugsley, "A critical evaluation of literature correlations for predicting bubble size and velocity in gas–solid fluidized beds," *Powder Technol.*, vol. 205, no. 1–3, pp. 1–14, Jan. 2011.

[7] R. C. Darton, R. D. LaNauze, J. F. Davidson, and D. Harrison, "Bubble growth due to coalesence in fluidised beds," *Trans Inst Chem Eng*, vol. 55, no. 4, pp. 274–280, 1977.

[8] D. Kunii and O. Levenspiel, *Fluidization Engineering*, Second. Butterworth-Heinemann, 1991.

[9] I. a. Abba, J. R. Grace, H. T. Bi, and M. L. Thompson, "Spanning the flow regimes: Generic fluidized-bed reactor model," *AIChE J.*, vol. 49, pp. 1838–1848, Jul. 2003.

[10] A. Mahecha-Botero, J. R. Grace, C. Jim Lim, S. S. E. H. Elnashaie, T. Boyd, and A. Gulamhusein, "Pure hydrogen generation in a fluidized bed membrane reactor: Application of the generalized comprehensive reactor model," *Chem. Eng. Sci.*, vol. 64, no. 17, pp. 3826–3846, 2009.

[11] I. A. Abba, "A Generalized Fluidized Bed Reactor Model Across The Flow Regimes," University of British Columbia, 2001.

[12] S. P. Sit and J. R. Grace, "Effect of bubble interaction on interphase mass transfer in gas fluidized beds," *Chem. Eng. Sci.*, vol. 36, no. 2, pp. 327–335, 1981.

[13] A. Vepsäläinen, S. Shah, J. Ritvanen, and T. Hyppänen, "Interphase mass transfer coefficient in fluidized bed combustion by Eulerian CFD modeling," *Chem. Eng. Sci.*, vol. 106, pp. 30–38, 2014.

[14] J. D. Murray, "On the mathematics of fluidization: Part 2. Steady motion of fully developed bubbles," *J. Fluid Math.*, vol. 22, pp. 57–80, 1965.

[15] E. N. Fuller, P. D. Schettler, and J. C. Giddings, "A new method for prediction of binary gas-phase diffusion coefficients.," *Ind. Eng. Chem.*, vol. 16, no. 10, p. 551, 1966.

[16] H. T. Bi, N. Ellis, I. A. Abba, and J. R. Grace, "A state-of-the-art review of gas-solid turbulent fluidization," *Chem. Eng. Sci.*, vol. 55, pp. 4789–4825, 2000.

[17] J. M. Matsen, "Fluidized Beds," in *Scale-up of chemical processes. In: Bisio, A., Kabel, R.L. (Eds.)*, John Wiley and Sons, 1985, pp. 347–405.

[18] G. S. Lee and S. D. Kim, "Axial mixing of solids in turbulent fluidized beds," *Chem. Eng. J.*, vol. 44, pp. 1–9, 1990.

[19] J. R. Grace, "Reflections on turbulent fluidization and dense suspension upflow," *Powder Technol.*, vol. 113, no. 3, pp. 242–248, 2000.

[20] M. Pell, *Handbook of Powder Technology - Gas Fluidization*. Amsterdam: Elsevier Science Publishers B.V., 1990.

[21] G. S. Patience, J. Chaouki, F. Berruti, and R. Wong, "Scaling considerations for circulating fluidized bed risers," *Powder Technol.*, vol. 72, no. 1, pp. 31–37, 1992.

[22] H. T. Bi, "Some Issues on Core-Annulus and Cluster Models of Circulating Fluidized Bed Reactors," *Can. J. Chem. Eng.*, vol. 80, no. October, pp. 809–817, 2002.

[23] T. S. Pugsley, G. S. Patience, F. Berruti, and J. Chaouki, "Modeling the catalytic oxidation of n-butane to maleic anhydride in a circulating fluidized bed reactor," *Ind. Eng. Chem. Res.*, vol. 31, no. 12, pp. 2652–2660, 1992.

[24] R. W. Breault, "A review of gas–solid dispersion and mass transfer coefficient correlations in circulating fluidized beds," *Powder Technol.*, vol. 163, no. 1–2, pp. 9–17, 2006.

[25] J. Chaouki, L. Godfroy, and F. Larichi, "Position and Velocity of a Large Particle in a GadSolid Riser using the Radioactive Particle Tracking Technique," *Can. J. Chem. Eng.*, vol. 77, pp. 253–261, 1999.

[26] F. Wei, Y. Jin, Z. Yu, and W. Chen, "Lateral and axial mixing of the dispersed particles in CFB," *J. Chem. Eng. Japan*, vol. 28, pp. 506–510, 1995.